

Low writing energy and sub nanosecond spin torque transfer switching of in-plane magnetic tunnel junction for spin torque transfer random access memory

H. Zhao, A. Lyle, Y. Zhang, P. K. Amiri, G. Rowlands, Z. Zeng, J. Katine, H. Jiang, K. Galatsis, K. L. Wang, I. N. Krivorotov, and J.-P. Wang

Citation: *Journal of Applied Physics* **109**, 07C720 (2011);

View online: <https://doi.org/10.1063/1.3556784>

View Table of Contents: <http://aip.scitation.org/toc/jap/109/7>

Published by the [American Institute of Physics](#)

Articles you may be interested in

[Perpendicular spin transfer torque magnetic random access memories with high spin torque efficiency and thermal stability for embedded applications \(invited\)](#)

Journal of Applied Physics **115**, 172615 (2014); 10.1063/1.4870917

[Spin torque switching of 20 nm magnetic tunnel junctions with perpendicular anisotropy](#)

Applied Physics Letters **100**, 132408 (2012); 10.1063/1.3694270

[Tunnel magnetoresistance of 604% at 300K by suppression of Ta diffusion in CoFeB / MgO / CoFeB pseudo-spin-valves annealed at high temperature](#)

Applied Physics Letters **93**, 082508 (2008); 10.1063/1.2976435

[Ultrafast switching in magnetic tunnel junction based orthogonal spin transfer devices](#)

Applied Physics Letters **97**, 242510 (2010); 10.1063/1.3527962

[Electric field-induced magnetization reversal in a perpendicular-anisotropy CoFeB-MgO magnetic tunnel junction](#)

Applied Physics Letters **101**, 122403 (2012); 10.1063/1.4753816

[Spin transfer torque devices utilizing the giant spin Hall effect of tungsten](#)

Applied Physics Letters **101**, 122404 (2012); 10.1063/1.4753947

Scilight

Sharp, quick summaries **illuminating**
the latest physics research

Sign up for **FREE!**



Low writing energy and sub nanosecond spin torque transfer switching of in-plane magnetic tunnel junction for spin torque transfer random access memory

H. Zhao,¹ A. Lyle,¹ Y. Zhang,¹ P. K. Amiri,² G. Rowlands,³ Z. Zeng,⁴ J. Katine,⁵ H. Jiang,⁴ K. Galatsis,² K. L. Wang,² I. N. Krivorotov,³ and J.-P. Wang^{1,a)}

¹Department of Electrical and Computer Engineering, University of Minnesota, Minneapolis, Minnesota 55455, USA

²Department of Electrical Engineering, University of California, Los Angeles, California 90095, USA

³Department of Physics and Astronomy, University of California, Irvine, California 92697, USA

⁴Department of Physics and Astronomy, University of California, Los Angeles, California 90095, USA

⁵Hitachi Global Storage Technologies, San Jose, California 95135, USA

(Presented 18 November 2010; received 24 September 2010; accepted 25 November 2010; published online 29 March 2011)

This work investigated in-plane MgO-based magnetic tunnel junctions (MTJs) for the application of spin torque transfer random access memory (STT-RAM). The MTJ in this work had an resistance area product (RA) = 4.3 $\Omega \cdot \mu\text{m}^2$, tunneling magnetoresistance ratio $\sim 135\%$, thermal stability factor $\Delta(H) = 68$ (by field measurement), and $\Delta(I) = 50$ (by current measurement). The optimal writing energy was found to be 0.286 pJ per bit at 1.54 ns for antiparallel (AP) state to parallel (P) state switching, and 0.706 pJ per bit at 0.68 ns for P state to AP state switching. Ultra fast spin torque transfer (STT) switching was also observed in this sample at 580 ps (AP to P) and 560 ps (P to AP). As a result, 0.6–1.3 GHz was determined to be the optimal writing rate from writing energy consumption of view. These results show that in-plane MgO MTJs are still a viable candidate as the fast memory cell for STT-RAM. © 2011 American Institute of Physics. [doi:10.1063/1.3556784]

Spin torque transfer random access memory (STT-RAM) is a very promising candidate for the next generation of mainstream universal memory.^{1–4} The key advantages of STT-RAM over competing technologies are its nonvolatile, high speed, and energy-efficient writing. MgO magnetic tunnel junctions as the basic memory cell in STT-RAM have been widely studied since 2004.^{5–8} However, most studies focus on separate aspects of the MTJ such as the TMR ratio, the critical current density, the thermal stability, or the switching mechanism, but not the MTJ as a whole for STT-RAM application. For real device design, this is impractical since all aspects should be balanced in order to integrate with CMOS (Refs. 2 and 4) and to perform as a reliable memory device. Among all those practical requirements, the writing energy and thermal stability of single MTJ bit are the key parameters in STT-RAM memory cell design.^{4,9} It is crucial to achieve low writing energy while maintaining reasonable thermal stability at the same time

In this paper, we investigated the in-plane MgO MTJ according to the STT-RAM application requirement and showed that it is a viable candidate for STT-RAM. Ultralow writing energy and ultrafast switching from both switching direction were observed. The switching probability distribution was measured from sub nanosecond to millisecond regime to analyze both the precessional and thermally activated switching modes.

The MTJ samples in this report were prepared using a Singulus sputtering system with a stacking structure of (bottom electrode)/PtMn (15 nm)/Co₇₀Fe₃₀ (2.5 nm)/Ru

(0.85 nm)/Co₄₀Fe₄₀B₂₀ (2.4 nm)/MgO (0.83 nm)/Co₆₀Fe₂₀B₂₀ (1.8 nm)/(top electrode). It was postannealed at 300 °C under 1 T magnetic field for 2 h. The wafer was then patterned into elliptical nanopillars with different sizes and aspect ratios. The results in this paper were measured in the same MTJ with the optimal size of 130 × 50 nm². Switching probability was measured in switching process both from antiparallel (AP) state to parallel (P) state and from parallel (P) state to antiparallel (AP) state. The whole measuring process is as follows (take the switching from AP to P as an example). The MTJ was first reset to AP state by applying a large external field about twice the free layer saturation field for 1 s. Then, the large reset field was replaced by a small bias field, which compensates the free layer offset field. Subsequently, a short voltage switching pulse was applied to the junction through ground signal ground (GSG) probe. Finally, the junction resistance was measured by applying a small dc readout current to determine whether it has switched or not. This sequence was repeated for 100 times to calculate the final switching probability under each condition.

Figure 1 shows the magnetoresistance minor loop for a 130 × 50 nm² MTJ sample. The tunneling magnetoresistance (TMR) ratio of this junction is 135%, free layer room temperature coercivity is 48 Oe, and resistance area (RA) product at P state is 4.3 $\Omega \cdot \mu\text{m}^2$. The abrupt switching in this R-H loop means the junction free layer acts as a single domain unit.

The switching probability as a function of pulse width and pulse amplitude is shown in Figs. 2(a) and 2(b). In this paper, the pulse amplitude is the mean pulse voltage on device which is calculated by $2V_{\text{incident}}R_{\text{MTJ}}/(R_{\text{MTJ}} + Z_0)$ due to the impedance mismatch in circuit. Z_0 is the circuit system

^{a)}Electronic mail: jpwang@umn.edu.

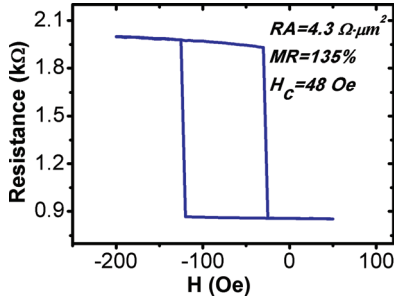


FIG. 1. (Color online) Resistance versus magnetic field loop of a MTJ with the size of $50 \times 130 \text{ nm}^2$.

impedance, 50Ω . Both the writing energy and switching time are defined at 50% switching probability corresponding to the dashed line in the figure. From the two figures, we can see that ultrafast switching around 0.5 ns is achievable when the pulse amplitude is about 1 V (purple curve and red curve). For AP to P switching, the measured shortest writing pulse width is 580 ps at 1.075 V , and for P to AP switching, the shortest writing pulse width is 560 ps at 1.048 V . Further increase of the pulse amplitude will reduce the switching time more; however, 1 V is already close to the breakdown voltage. So there is a large chance to short the thin MgO barrier with pulse above 1 V for this RA value.

The pulse amplitude and switching time is plotted in Figs. 2(c) and 2(d). In the nanosecond regime, the spin torque transfer switching is a precessional process. According to the Macrospin model,¹⁰ the switching speed is inversely proportional to the applied current,

$$\tau \propto \frac{\ln(\pi/2\theta_0)}{J - J_{c0}}, \quad (1)$$

where θ_0 is the initial angle between the free layer and the fixed layer while J and J_{c0} is the applied and intrinsic critical current densities, respectively. Therefore, the switching time is inversely proportional to the pulse voltage,

$$\tau^{-1} = A \times (V - V_{c0}). \quad (2)$$

We define V_{c0} as the intrinsic switching voltage. In the figure, the red dashed curve is the fitting curve according to the above formula. We can see the data fit well with this model in the regime from 0.5 to 6 ns in both figures, which is similar to other reports.¹¹ The fitting parameters are $A_{\text{ap-p}} = 2.14 \times 10^9 \text{ s}^{-1} \text{ V}^{-1}$ and $V_{c0 \text{ ap-p}} = 0.305 \text{ V}$ for AP to P switching, and $A_{\text{p-ap}} = 2.09 \times 10^9 \text{ s}^{-1} \text{ V}^{-1}$ and $V_{c0 \text{ p-ap}} = 0.363 \text{ V}$ for P to AP switching. Convert those values to critical current and critical current density as $I_{c0 \text{ ap-p}} = 0.152 \text{ mA}$, $J_{c0 \text{ ap-p}} = 2.98 \times 10^6 \text{ A/cm}^2$, and $I_{c0 \text{ p-ap}} = 0.427 \text{ mA}$, $J_{c0 \text{ p-ap}} = 8.37 \times 10^6 \text{ A/cm}^2$.

Now we can determine the minimum AP to P writing energy for a single bit from the correlation between switching pulse voltage and switching time. The writing energy is calculated by

$$E = V^2 \tau / R_{\text{MTJ}}. \quad (3)$$

Therefore, the writing energy equals

$$E = \frac{V^2 \tau}{R_{\text{MTJ}}} = \frac{(\frac{1}{A\tau} + V_{c0})^2 \tau}{R_{\text{MTJ}}}. \quad (4)$$

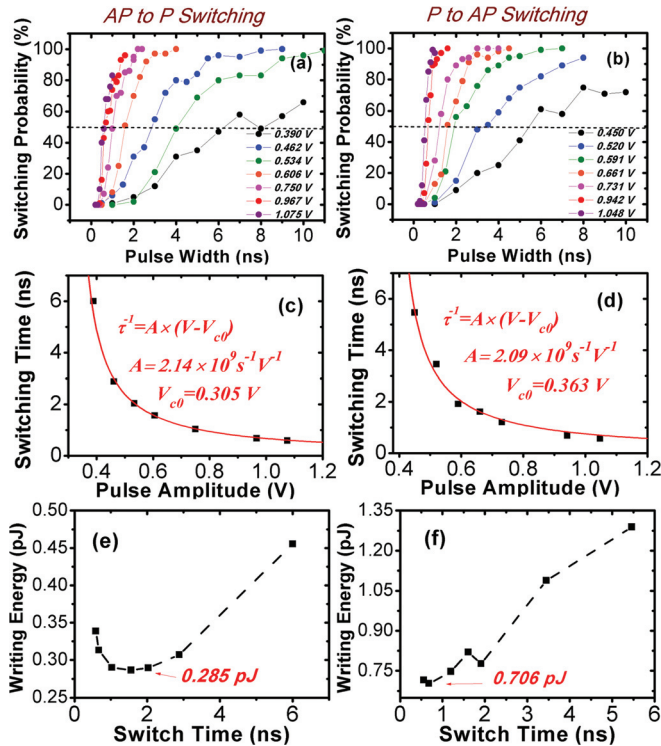


FIG. 2. (Color online) (a) and (b) Switching probability dependence on writing pulse width of different pulse amplitude; (c) and (d) switching time versus pulse amplitude at 50% switching probability; (e) and (f) writing energy dependence on switching time.

And it has the minimum when $\tau_{\text{ap-p}} = 1/AV_{c0\text{ap-p}} = 1.53 \text{ ns}$ or $\tau_{\text{p-ap}} = 1/AV_{c0\text{p-ap}} = 1.31 \text{ ns}$. The measured writing energy is shown in Figs. 2(e) and 2(f). A minimum writing energy is found at 1.56 ns for AP to P switching, and 0.68 ns for P to AP switching, which is in good agreement with the prediction. The optimal 50% switching probability writing energy is as low as 0.286 pJ for AP to P switching and 0.706 pJ for P to AP switching. Even for applications that require significantly low write error rates, the writing energy for 100% switching probability of this sample is still as low as 0.685 pJ (AP to P) and 1.67 pJ (P to AP). This result proves that very low writing energy consumption can be achieved with GHz writing rate in a simple in-plane MgO MTJ sample.

Furthermore, according to our measurement, we also found that the optimal writing energy is always obtained around 1 ns . For shorter writing time, the required pulse amplitude increases rapidly. And for longer writing time, the energy is wasted due to the extra time. As a result, $0.6\text{--}1.3 \text{ GHz}$ is proved to be the optimal writing rate from energy consumption point of view.

Based on the above switching probability data, we can plot the whole phase diagram of ns STT switching in Figs. 3(a) and 3(b). The switching probability distribution is shown by the color as labeled next to the figure. So in both figures, the blue color area represents a stable parallel state and red color area stands for a stable antiparallel state.

Between the two areas, there is a switching probability distribution from 0% to 100%.

For an in-plane MTJ, its writing energy is mainly determined by the in-plane magnetic anisotropy field. However, reducing the in-plane anisotropy field also means reducing the energy barrier, i.e., the thermal stability. Therefore, finding a balance between writing energy and thermal stability is critical for in-plane MTJ cell for STT-RAM application. It is important to maintain a relatively high thermal stability while pursuing low writing energy. The conventional thermal stability factor is defined as

$$\Delta(H) = K_v V_H / k_B T, \quad (5)$$

where K_v is the magnetic anisotropy, V_H is the volume of free layer, and $k_B T$ are the Boltzmann constant and temperature, respectively. It follows the classic thermal fluctuation theory

$$M = M_0 \exp \left[-\frac{t}{\tau_0} \exp \left(-\frac{K_u V_H}{k_B T} \right) \right]. \quad (6)$$

$\Delta(H)$ defines the maximum time that MTJ can keep its initial magnetic state after writing against thermal agitation. For 10 years data stabilization, it is required to be larger than 60.⁴ $\Delta(H)$ is also called the field switching delta since it does not include the effect on thermal stability of currents needed for current writing and reading. It was found that the current switching delta can be much smaller than the field switching delta.¹²

The thermal stability associated with STT current writing is defined as

$$\Delta(I) = K_v V_I / k_B T, \quad (7)$$

where V_I is the effective activation volume for STT current writing. It is defined by the STT thermal activation switching model

$$J_c(\tau) = J_{c0} \left[1 - \frac{k_B T}{K_u V_I} \ln \left(\frac{\tau}{\tau_0} \right) \right]. \quad (8)$$

The minimum current-induced switching delta to ensure low writing error rate is 40.⁴

In our sample, the field switching delta was tested by spin torque ferromagnetic resonance (ST-FMR) measurement. $\Delta(H)$ equals 68 for MTJs with $130 \times 50 \text{ nm}^2$ size. And $\Delta(I)$ is fitted by STT switching data according to Eq. (8) in STT thermal activation switching regime ($>10 \text{ ns}$). Both the short pulse switching and long pulse switching data are plot-

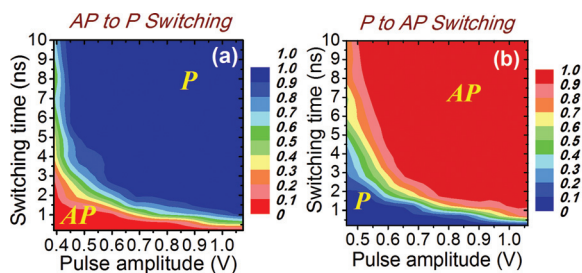


FIG. 3. (Color online) (a) and (b) Spin torque transfer switching phase diagram in nanosecond regime.

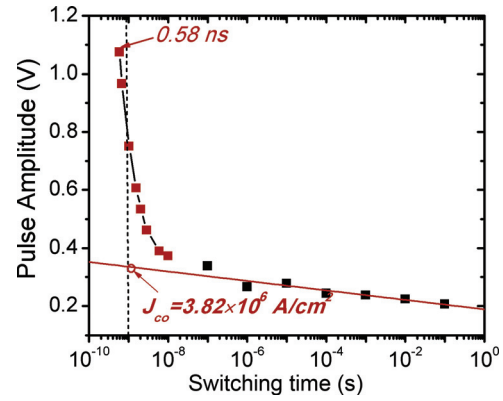


FIG. 4. (Color online) Switching time versus pulse amplitude at 50% switching probability from 0.5 ns to 0.1 s for AP to P switching. The red and black dots are experimental data, which follow the precessional switching model and thermal activation model, respectively. Red line is the thermal activation model fitting curve and vertical black dotted line is the guild line of 1 ns.

ted together in Fig. 4. Two distinct switching modes can be found in this figure. For short pulse, the current-induced switching follows precessional switching model as discussed in the previous section. While for the long pulse, the current-induced switching mainly follows the thermal activation model.^{10,13} From Fig. 4, it is clear that the experiment data agrees well with this model. $\Delta(I)$ is found to be 50. Also the intrinsic critical current density here is $J_{c0} = 3.82 \times 10^6 \text{ A/cm}^2$ from thermal activation model, close to our previous value $2.98 \times 10^6 \text{ A/cm}^2$ estimated from the precessional switching model.

In conclusion, we demonstrated the nanosecond and sub nanosecond current-induced switching of in-plane MgO MTJ for STT-RAM application. Considering the critical current of this sample is not among the lowest values of other reported in-plane MTJs, it is believed that the writing energy can be still reduced by further reducing the critical current. Although perpendicular MTJ holds its advantage at low I_{c0}/Δ ratio in theory, considering other advantages of in-plane MgO MTJ including high yield, we showed that it is still a good choice for STT-RAM before the mature of perpendicular MTJ cell.

This work was supported by the DARPA STT-RAM program. Y. Zhang and A. Lyle are supported by MRSEC Program of the National Science Foundation under Award Number DMR-0819885. J. P. Wang and H. Zhao are also grateful to the partial support from Intel and useful discussion with Dr. B. Doyle and Dr. Charles Kuo.

- ¹M. Hosomi *et al.*, *IEDM Tech. Dig.*, 459 (2005).
- ²T. Kawahara *et al.*, *ISSCC Tech. Dig.*, 480 (2007).
- ³C. J. Lin *et al.*, *IEDM Tech. Dig.*, 279, (2009).
- ⁴E. Chen *et al.*, *IEEE Trans. Magn.* **46**, 1873 (2010).
- ⁵S. Ikeda *et al.*, *IEEE Trans. Electron Devices* **54**, 991 (2007).
- ⁶S. Assefa *et al.*, *J. Appl. Phys.* **102**, 063901 (2007).
- ⁷J. Hayakawa *et al.*, *IEEE Trans. Magn.* **44**, 1962 (2008).
- ⁸T. Aoki *et al.*, *Appl. Phys. Lett.* **96**, 142502 (2010).
- ⁹H. Meng and J. P. Wang, *Appl. Phys. Lett.* **89**, 152909 (2006).
- ¹⁰J. Z. Sun, *Phys. Rev. B* **62**, 570 (2000).
- ¹¹D. Bedau *et al.*, *Appl. Phys. Lett.* **96**, 022514 (2010).
- ¹²T. Min *et al.*, *IEEE Tran. Magn.* **46**, 2322 (2010).
- ¹³J. Z. Sun, *IBM J. Res. Dev.* **50**, 81 (2006).